

Spin blockade with spin singlet electrons

Y. C. Sun, S. Amaha, S. M. Huang, J. J. Lin, K. Kono, and K. Ono

Citation: *Applied Physics Letters* **101**, 263108 (2012); doi: 10.1063/1.4773304

View online: <http://dx.doi.org/10.1063/1.4773304>

View Table of Contents: <http://scitation.aip.org/content/aip/journal/apl/101/26?ver=pdfcov>

Published by the [AIP Publishing](#)

Articles you may be interested in

[Electron Nuclear Spin Polarization Dynamics in InGaAs Quantum Dots](#)

AIP Conf. Proc. **1199**, 389 (2010); 10.1063/1.3295465

[Hysteretic behavior in weakly coupled double-dot transport in the spin blockade regime](#)

Appl. Phys. Lett. **91**, 252112 (2007); 10.1063/1.2828029

[Transport Properties of Strongly Correlated Electrons in Quantum Dots Using a Simple Circuit Model](#)

AIP Conf. Proc. **850**, 1384 (2006); 10.1063/1.2355222

[Nonequilibrium Electron Transport through Quantum Dots in the Kondo Regime](#)

AIP Conf. Proc. **850**, 1378 (2006); 10.1063/1.2355219

[Spin oscillation of a quantum dot embedded in a ferromagnetic ring with two interacting electrons](#)

J. Appl. Phys. **99**, 08F711 (2006); 10.1063/1.2177410

The advertisement features a dark blue background with white and orange text. At the top left, it reads 'NEW! Asylum Research MFP-3D Infinity™ AFM' in large white letters, followed by 'Unmatched Performance, Versatility and Support' in orange. On the right, the Oxford Instruments logo is shown in a white box, with the tagline 'The Business of Science®' below it. The central part of the ad is divided into four quadrants, each with an image and text: top-left shows a blue textured surface with the text 'Stunning high performance'; top-right shows a brown textured surface with 'Simpler than ever to GetStarted™'; bottom-left shows a patterned surface with 'Comprehensive tools for nanomechanics'; bottom-right shows a grid of small samples with 'Widest range of accessories for materials science and bioscience'. On the far right, there is a photograph of the MFP-3D Infinity AFM instrument.

Spin blockade with spin singlet electrons

Y. C. Sun,^{1,2} S. Amaha,¹ S. M. Huang,³ J. J. Lin,^{2,4} K. Kono,¹ and K. Ono^{1,a)}

¹Low Temperature Physics Laboratory, RIKEN, Wako, Saitama 351-0198, Japan

²Department of Electrophysics, National Chiao Tung University, Hsinchu 30010, Taiwan

³Department of Physics, National Sun Yat-Sen University, Kaohsiung 80424, Taiwan

⁴Institute of Physics, National Chiao Tung University, Hsinchu 30010, Taiwan

(Received 8 November 2012; accepted 10 December 2012; published online 28 December 2012)

We observe a singlet spin blockade (SSB) in two-electron vertical double quantum dots where the single-electron transport is blocked for spin singlet electrons. In contrast to the conventional Pauli spin blockade with spin triplet electrons, this singlet spin blockade is observed under high magnetic field, where the doubly occupied states in one of the dots go beyond the singlet-triplet ground-state transition. The SSB region in Coulomb diamond measurements is in agreement with the two-electron excitation spectrum. A leakage current of 10 pA order is observed in SSB, consistent with the spin singlet lifetime due to random nuclear spin fluctuations. © 2012 American Institute of Physics. [<http://dx.doi.org/10.1063/1.4773304>]

Pauli spin blockade (SB) in double quantum dots is one of the standard tools for accessing a single-electron spin via the electron transport. SB has been observed in various double dot structures, such as GaAs,^{1–4} Si dots,⁵ InAs nanowires,^{6,7} and nanocarbon materials,^{8,9} and has been used for initializing/measuring electron spin qubits,^{4,7,10} detecting hyperfine and/or spin-orbit-related electron spin scattering,^{1–3,6,9} and polarizing/measuring the collective nuclear spins in quantum dots.^{3,11}

SB is ubiquitously observed in series-connected double quantum dots with the current-carrying charge cycle of $(N_1, N_2) = (1, 1) \rightarrow (0, 2) \rightarrow (0, 1) \rightarrow (1, 1) \rightarrow \dots$, where N_1/N_2 is the number of electrons in the first/second dot.¹² In $(0, 2)$ states, at zero or small magnetic fields, two electrons occupy the same ground-state orbit, $1s$, and their spins are singlet, S . A spin triplet, $(0, 2)T$ has much higher energy, where two electrons occupy $1s$ and the second lowest orbit, $2p^+$.^{13,14} Thus, if two $(0, 2)$ states are appropriately tuned so that $(0, 2)S$ is within the transport window while $(0, 2)T$ is outside of it, they act as a spin-dependent barrier for nearly spin degenerated $(1, 1)$ states, i.e., they accept electrons tunnelling from $(1, 1)S$, but reject those from $(1, 1)T$ (Ref. 12) (see Fig. 1(a)).

A single quantum dot with two electrons has been known to show the singlet-triplet ground-state transition in magnetic field.^{13–16} A magnetic field B , applied perpendicular to the two-dimensional (2D) plane of a quantum dot, gives an additional confinement and increases the Coulomb energy for electrons sharing the $1s$ orbit (with a spin singlet). At the same time, the energy of the $2p^+$ orbit decreases, because its angular momentum is favored in the field. Thus, at a certain magnetic field, the two electrons eventually change their occupation from $1s^2$ to $1s2p^+$ (S - T transition). Owing to the exchange Coulomb interaction between electrons in $1s$ and $2p^+$, the spin triplet is the ground state for $1s2p^+$. In vertical quantum dots with a 2D harmonic confinement of ~ 5 meV, the ground-state transition occurs at the magnetic field of ~ 5 T, and the exchange splitting between

the $1s2p^+$ triplet state and $1s2p^+$ singlet excited state is ~ 2.5 meV.^{14,16} In $\text{In}_{0.05}\text{Ga}_{0.95}\text{As}$ vertical quantum dots, Zeeman splitting of triplet spin is minor in energy compared with the S - T transition.

In this letter, we demonstrate a singlet spin blockade (SSB), where the electron transport is blocked while leaving spin singlet electrons in the double dots. This singlet spin blockade takes place at high magnetic field beyond the singlet-triplet ground-state transition of $(0, 2)$ states, where the $(0, 2)$ state now accepts electrons tunneling from $(1, 1)T$ but not from $(1, 1)S$ (Fig. 1(b)).

We use a vertical double-quantum-dot device¹⁷ composed of 12-nm-thick $\text{In}_{0.05}\text{Ga}_{0.95}\text{As}$ wells with the outer/center barriers of 7-nm-/8-nm-thick $\text{Al}_{0.22}\text{Ga}_{0.78}\text{As}$. Two electrically independent Schottky gate electrodes surrounding dots can be used to tune the relative energy of two dots with left/right gate voltages, V_{gL}/V_{gR} . Source-drain current, I_{sd} , is measured at an effective electron temperature ~ 0.6 K. External magnetic fields are applied perpendicular to the barriers. For a given magnetic field, two gate voltages are carefully tuned, so that $(1, 1)$ and the $(0, 2)$ ground state are aligned at source-drain voltage $V_{sd} = 0$.^{11,18,19}

Figure 1(c) shows the $(0, 2)$ ground and excitation energy spectrum measured by sweeping gate voltages, V_g , under various magnetic fields from 0 to 10 T with fixed $V_{sd} = -4$ mV. The $1s^2(0, 2)S$ state (indicated by the solid line) and the $1s2p^+(0, 2)T$ state (dashed line) are clearly resolved and show the ground-state transition at 5 T.^{13,14} Another excited state appears for $B > 7$ T (dotted line), and undergoes the second ground-state transition at 9 T. This state is suggested to be the spin singlet state with high angular momentum.²⁰ Energy difference between the triplet ground state and the singlet excited state becomes maximum at ~ 7.5 T. Zeeman splitting was not observed owing to the expected small g-factor of our device. All these behaviors are consistent with previous measurement results of vertical single-dot devices.^{13,14}

Figure 1(d) shows Coulomb diamonds in an intensity plot of differential conductance, dI_{sd}/dV_{sd} , at zero magnetic field. Zero-current regions are colored white. SB appears on

^{a)}Electronic mail: k-ono@riken.jp.

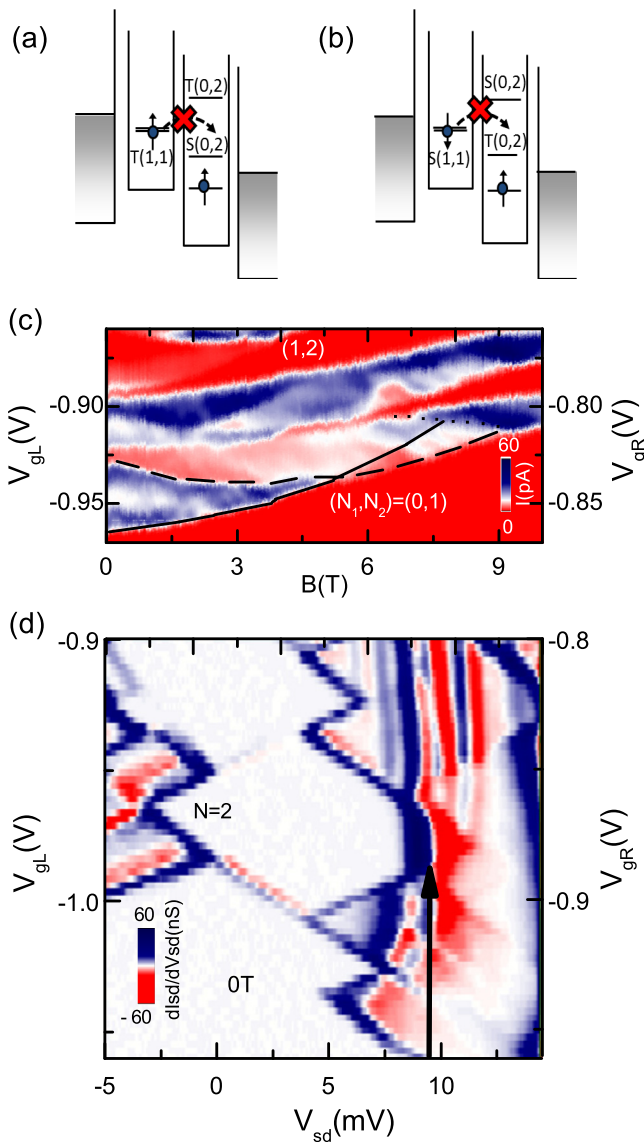


FIG. 1. Schematic diagrams for the mechanism of (a) a conventional Pauli spin blockade and (b) a singlet spin blockade. (c) Excitation energy spectrum for (0,2) states, measured at $V_{sd} = -4$ mV. The first current strip exhibits the (0,2) state evolution among the solid line of the $1s^2(0,2)S$ state, the dashed line of the $1s2p^+(0,2)T$ state, and the dotted line for another (0,2) S state. (d) $V_{sd} - V_g$ charge diagram at $B = 0$ T. SB is relieved at V_{sd} , indicated with an arrow, where the transition channel from (1,1) T to (0,2) T opens.

the positive V_{sd} side of the total electron number $N = 2$ Coulomb diamond. The right corner of the SB diamond is partially cut by a current threshold that runs nearly parallel to the vertical axis and is indicated by an arrow. Under this condition, a current-carrying cycle for triplet states takes place: $(1, 1)T \rightarrow (0, 2)T \rightarrow (0, 1) \rightarrow \dots$. Note that in Figs. 1(d) and 2(a)–2(c), a “current peak line” appears at two borders: between the SB region and $N = 1$ Coulomb blockade region and between the SB region and $N = 3$ Coulomb blockade region. On these two borders, (1,1) T is aligned with the Fermi energies of the source and drain electrodes, respectively, and SB is relieved. We have tuned V_{gL}/V_{gR} so that the current peak lines touch $V_{sd} = 0$ in the dI_{sd}/dV_{sd} plot.

We measured the Coulomb diamond data for various magnetic fields from 0 to 9 T. Figures 2(a)–2(f) show data taken before, during, and after the S - T transition. Increasing

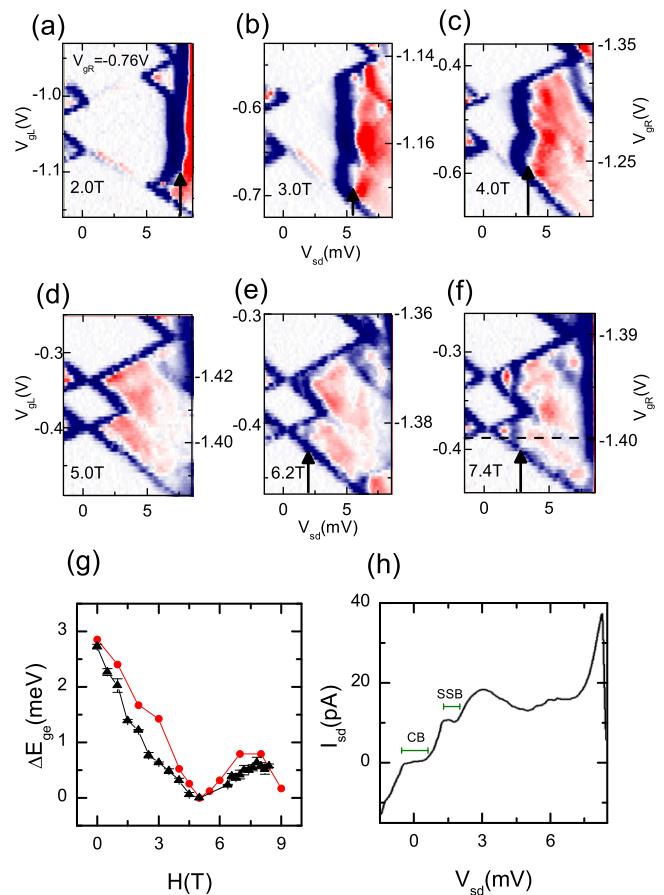


FIG. 2. dI_{sd}/dV_{sd} plots under the magnetic fields of (a) 2.0 T, (b) 3.0 T, (c) 4.0 T, (d) 5.0 T, (e) 6.2 T, and (f) 7.4 T. Scales are the same as in Fig. 1(d). The arrows mark the threshold of SB/SSB. At 5.0 T, SB is completely relieved and only the Coulomb blockade region is left. (g) Plots of energy difference between the ground and excited (0,2) states, ΔE_{ge} . Circles indicate data extracted from Fig. 1(c), and triangles are data from the series of Coulomb diamond measurements shown in (a)–(f). ΔE_{ge} measured as V_{gL}/V_{gR} (Fig. 1(c)) and V_{sd} ((a)–(f)) are converted to energy using the voltage drop ratio of three tunneling barriers. (h) $I_{sd} - V_{sd}$ curve along the dashed line in (f). A leakage current of 10 pA is observed in the SSB region.

the magnetic field yet further before the S - T transition, the current threshold due to $(1, 1)T \rightarrow (0, 2)T$ tunnelings (indicated with arrows in Figs. 2(a)–2(c)) shifts to lower V_{sd} , and the area for SB is decreased. At 5.0 T, near the S - T transition, the SB region completely disappears and leaves only the $N = 2$ Coulomb blockade region. Here, both (1,1) S and (1,1) T can tunnel into (0,2) states. At higher magnetic fields, after the S - T transition, Coulomb diamond data again show the current threshold, which implies tunneling into an (0,2) excited state (indicated by arrows in Figs. 2(e) and 2(f)). We observed that the current threshold shifts to higher V_{sd} with further increasing magnetic field. However, this threshold becomes blurred and difficult to trace for $B > 8.4$ T.

The (0,2) excitation spectrum (Fig. 1(c)) and V_{sd} values at the current threshold (Figs. 2(a)–2(f)) both give the magnetic-field-dependent energy difference between the ground and excited (0,2) states, ΔE_{ge} .^{12,13} The two results are summarized in Fig. 2(g) using circles and triangles, respectively; the results are nearly identical. This agreement confirms that SSB can take place in the range below the current threshold under $B > 5$ T. For this comparison of ΔE_{ge} , we first convert

the difference in the vertical V_g axis in Fig. 1(c) to V_{sd} ; then, both values from eV_g and eV_{sd} at the current threshold are multiplied by the voltage drop proportion on the barriers, estimated from the slopes of Coulomb diamonds.

Figure 2(h) shows the $I_{sd} - V_{sd}$ curve measured along the dashed line in Fig. 2(f). The current step at $V_{sd} \sim 3$ mV is the tunneling threshold for the first excited (0,2) state. The “leakage current” of ~ 10 pA is seen between the Coulomb blockade region and the threshold. Although the order of the current level is the same as the one above the threshold (~ 15 pA), we consider this value of leakage current to be consistent with SSB. In the SSB region, the blocked (1,1) S is nearly degenerated with one of the unblocked triplets, (1,1) T_0 , where T_0 is the zero component of triplet states. In the presence of the hyperfine interaction, nuclear spins generate a randomly fluctuating effective magnetic field ΔB_{nuc} (~ 10 mT for 10^5 nuclei in our dots) that can mix (1,1) S and (1,1) T_0 if their energy difference is smaller than the effective nuclear Zeeman energy by ΔB_{nuc} . The (1,1) $S - (1,1)T$ energy difference near zero magnetic field was estimated to be 0.42 to 0.83 μ eV using double-dot devices with similar barrier thicknesses.²¹ Thus, the hyperfine induced mixing is dominant in our devices. The time required for the mixing was measured in the lateral double quantum dots to be ~ 10 ns.² Our leakage current of 10 pA suggests that the average tunneling interval is $e/(10 \text{ pA}) \sim 10$ ns, where e is the elementary charge. This is consistent with the expected lifetime of (1,1) S . The smaller interdot tunnel barrier, less than the 8 nm in our system, will lift the degeneracy of the (1,1) S and (1,1) T_0 states and will decrease the leakage current in SSB.

We observe the SSB in two-electron charge diagrams of a vertical double-quantum-dot system, where the (0,2) state takes the spin triplet as the ground state under high magnetic field. The source-drain voltage dependences of the current threshold from the SB and SSB regions are consistent with the measured magnetic field dependence of the excitation spectrum of the (0,2) states. The leakage current found in SSB gives the lifetime of $S(1,1) \sim 10$ ns restricted by the randomly fluctuating effective magnetic field owing to the hyperfine interaction.

The authors thank H. Akimoto, M. Kawamura, and R. Takahashi for the assistance in experiments. The work was supported by RIKEN-NCTU Joint Graduate School

Program, JSPS KAKENHI Grant No. 11004535 and the Taiwan NSC through Grant No. NSC 100-2120-M-009-008.

- ¹A. C. Johnson, J. R. Petta, J. M. Taylor, A. Yacoby, M. D. Lukin, C. M. Marcus, M. P. Hanson, and A. C. Gossard, *Nature* **435**, 925 (2005).
- ²J. R. Petta, A. C. Johnson, J. M. Taylor, E. A. Laird, A. Yacoby, M. D. Lukin, C. M. Marcus, M. P. Hanson, and A. C. Gossard, *Science* **309**, 2180 (2005).
- ³J. Baugh, Y. Kitamura, K. Ono, and S. Tarucha, *Phys. Rev. Lett.* **99**, 096804 (2007); *Phys. Status Solidi C* **5**, 302 (2008).
- ⁴M. Pioro-Ladrière, T. Obata, Y. Tokura, Y.-S. Shin, T. Kubo, K. Yoshida, T. Taniyama, and S. Tarucha, *Nat. Phys.* **4**, 776 (2008).
- ⁵H. W. Liu, T. Fujisawa, Y. Ono, H. Inokawa, A. Fujiwara, K. Takashina, and Y. Hirayama, *Phys. Rev. B* **77**, 073310 (2008); N. S. Lai, W. H. Lim, C. H. Yang, F. A. Zwanenburg, W. A. Coish, F. Qassemi, A. Morello, and A. S. Dzurak, *Sci. Rep.* **1**, 110 (2011).
- ⁶A. Pfund, I. Shorubalko, K. Ensslin, and R. Leturcq, *Phys. Rev. Lett.* **99**, 036801 (2007); *Phys. Rev. B* **76**, 161308(R) (2007).
- ⁷S. Nadj-Perge, S. M. Frolov, E. P. A. M. Bakkers, and L. P. Kouwenhoven, *Nature* **468**, 1084 (2010).
- ⁸M. R. Buitelaar, J. Fransson, A. L. Cantone, C. G. Smith, D. Anderson, G. A. C. Jones, A. Ardavan, A. N. Khlobystov, A. A. R. Watt, K. Porfyrakis, and G. A. D. Briggs, *Phys. Rev. B* **77**, 245439 (2008).
- ⁹S. J. Chorley, G. Giavaras, J. Wabnitz, G. A. C. Jones, C. G. Smith, G. A. D. Briggs, and M. R. Buitelaar, *Phys. Rev. Lett.* **106**, 206801 (2011).
- ¹⁰F. H. L. Koppens, C. Buizert, K. J. Tielrooij, I. T. Vink, K. C. Nowack, T. Meunier, L. P. Kouwenhoven, and L. M. K. Vandersypen, *Nature* **442**, 766 (2006).
- ¹¹R. Takahashi, K. Kono, S. Tarucha, and K. Ono, *Phys. Rev. Lett.* **107**, 026602 (2011).
- ¹²K. Ono, D. G. Austing, Y. Tokura, and S. Tarucha, *Science* **297**, 1313 (2002).
- ¹³L. P. Kouwenhoven, T. H. Oosterkamp, M. W. S. Danoesastro, M. Eto, D. G. Austing, T. Honda, and S. Tarucha, *Science* **278**, 1788 (1997).
- ¹⁴W. G. van der Wiel, T. H. Oosterkamp, J. W. Janssen, L. P. Kouwenhoven, D. G. Austing, T. Honda, and S. Tarucha, *Physica B* **256**, 173 (1998).
- ¹⁵R. C. Ashoori, H. L. Stormer, J. S. Weiner, L. N. Pfeiffer, K. W. Baldwin, and K. W. West, *Phys. Rev. Lett.* **71**, 613 (1993); T. Schmidt, M. Tewordt, R. H. Blick, R. J. Haug, D. Pfannkuche, K. v. Klitzing, A. Förster, and H. Lüth, *Phys. Rev. B* **51**, 5570 (1995).
- ¹⁶M. Eto, *Jpn. J. Appl. Phys., Part 1* **38**, 376 (1999).
- ¹⁷D. G. Austing, T. Honda, and S. Tarucha, *Jpn. J. Appl. Phys., Part 1* **36**, 1667 (1997).
- ¹⁸R. Hanson, L. P. Kouwenhoven, J. R. Petta, S. Tarucha, and L. M. K. Vandersypen, *Rev. Mod. Phys.* **79**, 1217 (2007).
- ¹⁹F. H. L. Koppens, J. A. Folk, J. M. Elzerman, R. Hanson, L. H. Willems van Beveren, I. T. Vink, H. P. Tranitz, W. Wegscheider, L. P. Kouwenhoven, and L. M. K. Vandersypen, *Science* **309**, 1346 (2005).
- ²⁰M. Wagner, U. Merkt, and A. V. Chaplik, *Phys. Rev. B* **45**, 1951 (1992).
- ²¹T. Kodera, K. Ono, Y. Kitamura, Y. Tokura, Y. Arakawa, and S. Tarucha, *Phys. Rev. Lett.* **102**, 146802 (2009).